

*Work supported in part by the French Direction des Recherches et Moyens d'Essais, Ministère des Armées under Contract No. 74-198 and Centre National de la Recherche Scientifique under Contract No. ATP 1215-1V02.

¹J. H. Dinan, L. K. Galbraith, and T. E. Fischer, *Surf. Sci.* **26**, 587 (1971).

²D. E. Eastman and W. D. Grobman, *Phys. Rev. Lett.* **28**, 1378 (1972).

³P. E. Gregory, W. E. Spicer, S. Ciraci, and W. A. Harrison, *Appl. Phys. Lett.* **25**, 511 (1974).

⁴P. E. Gregory and W. E. Spicer, *Phys. Rev. B* **13**, 725 (1976).

⁵D. E. Eastman and J. L. Freeouf, *Phys. Rev. Lett.* **33**, 1601 (1974).

⁶J. Van Laar and J. J. Scheer, *Surf. Sci.* **8**, 342 (1967).

⁷A. Huijser and J. Van Laar, *Surf. Sci.* **52**, 202 (1975).

⁸G. M. Guichar, C. Sebenne, G. Garry, and M. Balkanski, *Le Vide, Les Couches Minces* **30A**, 97 (1975).

⁹G. M. Guichar, C. A. Sebenne, G. A. Garry, and M. Balkanski, to be published.

¹⁰Usually, one says that the Fermi level is pinned when the work function does not change with the doping level and type. It is almost the case for silicon but, for GaAs, the work function is well known to depend on the type and the word "pinning" seems inappropriate.

¹¹R. Dorn, H. Lüth, and G. J. Russel, *Phys. Rev. B* **10**, 5049 (1974).

¹²R. Ludeke and L. Esaki, *Phys. Rev. Lett.* **33**, 653 (1974).

¹³A. R. Lubinsky, C. B. Duke, B. W. Lee, and P. Mark, *Phys. Rev. Lett.* **36**, 1058 (1976).

¹⁴Clean cleaved silicon (111) usually exhibits a 2×1 superstructure but it has been reported [J. E. Rowe, S. B. Christman, and H. Ibach, *Phys. Rev. Lett.* **34**, 87 (1975)] that one-half order LEED spots are no longer seen for cleavages with high step density suggesting reconstruction is inhibited for terrace widths less than 40–50 Å.

Experimental Test of Renormalization Group Theory on the Uniaxial, Dipolar Coupled Ferromagnet LiTbF₄

J. Als-Nielsen

Research Establishment Risø, DK-4000 Roskilde, Denmark

(Received 7 July 1976)

The transverse correlation range ξ and the susceptibility in the critical region has been measured by neutron scattering. A special technique required to resolve the superdiverging longitudinal correlation range has been utilized. The results for ξ together with existing specific-heat data are in remarkable agreement with the renormalization group theory of systems with marginal dimensionality. The ratio between the susceptibility amplitudes above and below T_c was found to be 2 in accordance with renormalization-group and mean-field theory.

A simple, heuristic argument,¹ as well as renormalization-group analysis,² predicts that mean-field theory gives the correct critical behavior of phase transitions when the dimensionality d is larger than $d^*=4$, provided that the interaction is of short range. For the uniaxial dipolar-coupled ferromagnet it turns out^{3,4} that the marginal dimensionality is $d^*=3$. This may be understood in simple terms by considering the mean-field expression for the wave-vector-dependent susceptibility $\chi(\vec{q}, T)$ in the long wavelength limit,⁴

$$\chi^{-1}(\vec{q}, T) \propto 1 + \xi^2 [q^2 + g(q_z/q)^2 - hq_z^2]. \quad (1)$$

The parameter h approaches zero near T_c , and the hq_z^2 term is neglected in the following. The half-contour of $\chi(\vec{q}, T)$ in the q_x - q_z plane is shown in Fig. 1, the z direction being the Ising axis. The remarkable feature is that the longitudinal correlation range ξ_{\parallel} is superdiverging since it

varies as the *square* of the diverging transverse correlation range ξ . The volume of a region of correlated spins is therefore ξ to the power of

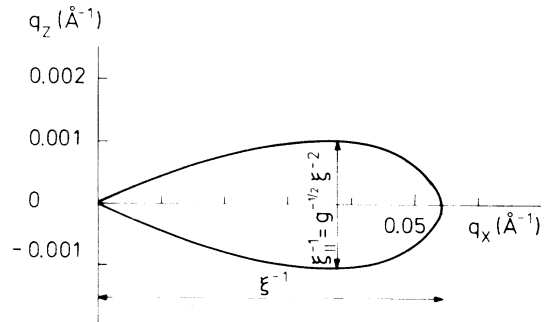


FIG. 1. The half-contour defined by $\chi(q_x, 0, q_z) = \frac{1}{2}\chi(q_x \rightarrow 0, 0, 0)$ 1% above the critical temperature. Note the factor of 10 between the q_x and q_z scales. The longitudinal correlation range ξ_{\parallel} varies as the square of the transverse correlation range ξ .

four rather than the cube of ξ , as it is for isotropic 3d systems; and this implies that the uniaxial dipolar-coupled ferromagnet displays marginal dimensionality in its critical behavior.

At $d=d^*$ the renormalization-group (RG) equations can be solved exactly, yielding logarithmic corrections to the mean-field behavior. Experiments on $d=d^*$ systems provide, therefore, an important test of RG theory.

Some time ago it was discovered that LiTbF_4 is very close to being a model system of the uniaxial dipolar-coupled ferromagnet⁵—a conclusion that was confirmed soon afterwards by detailed neutron scattering experiments,^{6,7} a technique by which the wave-vector-dependent susceptibility can be determined directly. However, the anomalous collapse of $\chi(\vec{q}, T)$ into the q_x - q_y plane as the critical temperature is approached demands an extreme q_z resolution as well as a perfect single crystal in order to measure the critical fluctuations precisely; and it is not until now that we have succeeded in meeting these requirements as will be explained below. On the other hand, measurements of the magnetization⁸ and of the specific heat⁹ can be carried out by conventional methods. This specific-heat data are of particular interest because the leading singularity is the logarithmic singularity. Ahlers, Kornblitt, and Guggenheim⁹ were able to show that the specific heat C at a reduced temperature $t = T/T_c - 1$ is consistent with the form

$$C/k_B = A_{\pm} |\ln t|^z \quad (2)$$

with $z = \frac{1}{3}$ and with the ratio A_+/A_- of the amplitudes above and below T_c equal to $\frac{1}{4}$ as predicted by RG theory. The magnetization data,⁸ measured by magnetic Bragg scattering of neutrons, are consistent with the RG prediction¹⁰

$$(M/M_0)^2 = B |t| |\ln t|^{2/3}. \quad (3)$$

Finally, the correlation range ξ is expected to obey⁴

$$\xi^2 = \Gamma_{\pm} |t|^{-1} |\ln t|^{1/3} \quad (4)$$

with the ratio Γ_+/Γ_- being equal to the mean-field value of 2. Most interestingly, Aharony and Halperin have recently shown¹¹ that the RG equations imply the mean-field relation between the specific heat, magnetization, and susceptibility³

$$t^2 T_c C \chi / M^2 = \frac{1}{3} \quad (5)$$

and furthermore the following nontrivial relation

between correlation range and specific heat:

$$\xi^2 \xi_{\parallel} C t^2 / k_B = (3/32\pi) |\ln t|. \quad (6)$$

Accurate data for the correlation range together with the existing specific-heat data⁹ would thus allow a crucial test of RG theory. We shall see in this Letter that the predictions of RG theory are verified quite accurately by the experiments.

We shall now give the main results of the experiment; details will be published shortly in a full article.¹² Figure 2 shows the temperature dependence of $\chi(\vec{q}, T)$ as measured by small-angle scattering of cold neutrons. At small scattering angles it may be shown¹² that the q resolution for elastic scattering is confined to the direction of the scattering vector, so with the scattering vector perpendicular to the Ising axis the resolution width along q_z is extremely small. Cold neutrons were employed in order to reduce the q_x, q_y resolution widths. The crystal was enriched in the Li^7 isotope to minimize neutron absorption.

At constant wave-vector transfer $\vec{q} = (q_x, 0, 0)$, the intensity has a maximum at a temperature which we identify as the critical temperature T_c . Magnetic Bragg scattering from the $(0, 3, 1)$ re-

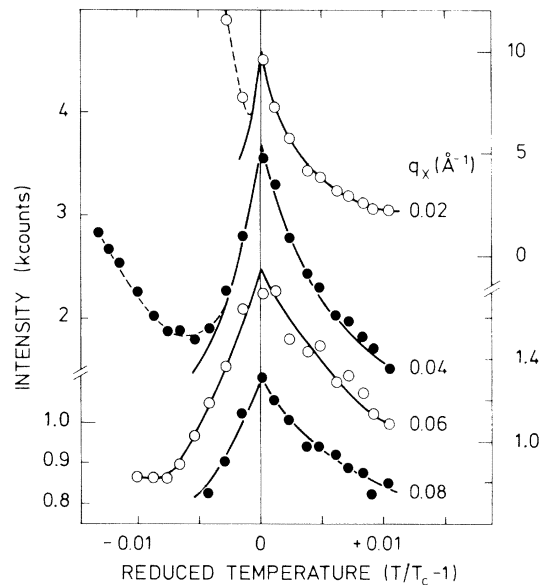


FIG. 2. Critical scattering versus temperature at fixed wave vector $q = (q_x, 0, 0)$. The asymmetric shape with a ratio of 2:1 between equicritical scattering above and below T_c is in accordance with mean-field and RG theory. The rise of intensity at low temperatures (dashed curve) is due to domain scattering. Left scales refer to filled signatures; right scales to open signatures.

flection⁸ yielded the same critical temperature to within 0.5 mK. The temperature scale in Fig. 2 is the reduced temperature $t = T/T_c - 1$. By inspection, it is immediately apparent that the intensity above T_c , $\chi(q, T)$, equals the intensity below T_c at half the reduced temperature, $\chi(q, t) = \chi(q, -t/2)$, in accordance with the expected amplitude ratio of $\Gamma_+/ \Gamma_- = 2$ in Eq. (4). This result is insensitive to systematic errors in the assessment of background or the resolution correction. In contrast, the ratio Γ_+/ Γ_- for the isotropic short-range-interaction Ising system such as β -brass is about¹³ 5.5. At the smaller wave vectors the intensities rise again at low temperatures. This contribution is not due to critical fluctuations but to diffraction from the growing domains of long-range order. The domains are long rods along the z axis; and, correspondingly, the scattering decreases very rapidly with q_z at constant q_x . As a matter of fact, we measured the q_z width to only 0.00012 \AA^{-1} full width at half-maximum (FWHM) at $q_x = 0.015 \text{ \AA}^{-1}$ and $t = -0.019$. This result shows unambiguously that the q_z resolution in small-angle elastic scattering (including the mosaic width of the sample crystal) is extremely small, so it is only the resolution in the q_x and q_y components that affects the critical scattering above T_c . By using tight collimations both in the vertical and horizontal directions, the resolution widths were 0.0062 and 0.030 \AA^{-1} FWHM along the q_x and q_y directions, respectively. The resulting resolution correction to the intensity data were less than 10% for almost all data points.

Scans along the q_z axis for fixed q_x near T_c were used to determine the parameter g in Eq. (1). When ξ is large, it is easily seen from Eq. (1) that the q_z width is $2g^{-1/2}q_x^2$ FWHM. Scans with q_z varying from 0.02 to 0.10 \AA^{-1} yielded $g = 1.3 \pm 0.1 \text{ \AA}^{-2}$ at T_c and 1% above T_c . This should be compared to the high-temperature mean-field value⁷ of $g = 1.56 \text{ \AA}^{-2}$. The results for ξ^2 versus $T/T_c - 1$ are shown in Fig. 3. These results were obtained from q_x scans with $q_z = 0$ by fitting a scale factor and ξ to the resolution-corrected and background-corrected intensities at each temperature.

Since experiments are not carried out in the ultimate asymptotic region, Aharony and Halperin suggested that in comparing RG theory with experiments the logarithm $|\ln t|$ in Eqs. (2)–(4) should be substituted by $|\ln t/t_0|$ with t_0 being a fit parameter. Indeed, the specific-heat data were analyzed in this way with the result of A/k_B

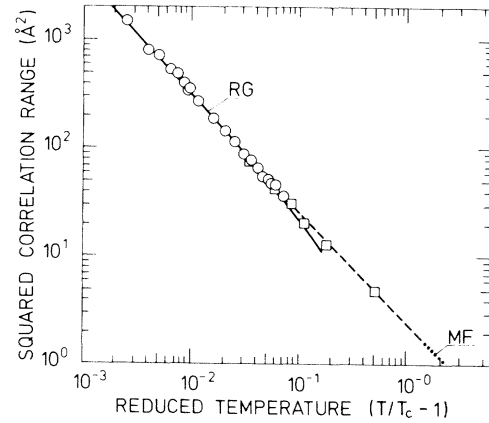


FIG. 3. The square of the correlation range ξ^2 versus the reduced temperature $t = (T/T_c - 1)$. The full line RG represents the prediction of renormalization-group theory $\xi^2 = 2.09t^{-1} |\ln t / 0.315|^{1/3} \text{ \AA}^2$. The dotted curve MF represents the mean-field behavior and the dashed line is a guide-to-the-eye interpolation between RG and MF. Circles are data obtained with tight collimation; squares are data with relaxed resolution.

$= 5.975 \times 10^{-3} \text{ \AA}^{-3}$ and $t_0 = 0.315$. Inserting these values in Eq. (6) and using $\xi_{||} = g^{1/2} \xi^2$ with the experimental value of $g = 1.30 \text{ \AA}^{-2}$, we find that RG theory predicts $\xi^2 = 2.09t^{-1} |\ln t / t_0|^{1/3} \text{ \AA}^2$, as shown by the full line in Fig. 3.

The agreement, with *no adjustable* parameters, between RG theory and specific-heat data on the one side and the neutron scattering data for the correlation range on the other side is remarkably good—as a matter of fact, it is difficult to imagine any other smooth curve fitting the data better in the interval of $0.002 < t < 0.060$ than the RG theory! The agreement between RG theory and experiment is quantitatively expressed by the value of $\chi^2 = 1.01$ in a χ^2 test. For comparison $\chi^2 = 147$ using the mean-field expression $\xi^2 = \xi_0^2 t^{-2\nu}$ with $\gamma = \frac{1}{2}$ and $\xi_0^2 = -C_4/C_3 = 1.352$ with the notation of Ref. 7. If we fit ξ_0 instead of using the dipolar mean-field value, we find ξ_0^2 (best fit) $= 2.90 \text{ \AA}^2$ with $\chi^2 = 4.8$.

The high-temperature behavior of ξ^2 is given⁷ by the dotted curve in Fig. 3. Below $2.5T_c$ this curve is joined to the semiasymptotic critical curve by a dashed line as an interpolation.

We have also attempted to compare the experimental results with Eq. (5), but rather large uncertainties are involved in determining χ/χ^0 on an absolute scale. Within the estimated systematic errors of 15% we find agreement with Eq. (5).

It would be misleading to conclude that we have observed logarithmic corrections to the mean-field behavior of the correlation range. However,

the specific-heat data together with our correlation-range data verify very accurately numerous predictions of renormalization-group theory: (a) A logarithmic singularity to the expected power of $\frac{1}{3}$ was clearly observed in the specific-heat data of Ahlers, Kornblitt, and Guggenheim. (b) The ratios between the amplitudes above and below T_c for the specific heat and for the susceptibility are 1:4 and 2:1, respectively. (c) The RG relation between the correlation range and specific heat has been confirmed to an accuracy of the order of 2%.

¹See, e.g., L. P. Kadanoff, in *Phase Transitions and Critical Phenomena*, edited by C. Domb and M. S. Green (Academic, New York, 1976), Vol. 5A, p. 18.

²K. G. Wilson and J. Kogut, *Phys. Rep.* **12C**, 75 (1974).

³A. I. Larkin and D. E. Khmel'nitzkii, *Zh. Eksp. Teor. Fiz.* **56**, 2087 (1969) [*Sov. Phys. JETP* **29**, 1123 (1969)].

⁴A. Aharony, *Phys. Rev. B* **8**, 3363 (1973), **9**, 3946 (1974).

⁵L. M. Holmes, T. Johansson, and H. J. Guggenheim, *Solid State Commun.* **12**, 993 (1973).

⁶L. M. Holmes, H. J. Guggenheim, and J. Als-Nielsen, in *Proceedings of the Ninth International Conference on Magnetism, Moscow, U. S. S. R., 1973* (Nauka, Moscow, U. S. S. R., 1974), Vol. VI, p. 256.

⁷J. Als-Nielsen, L. M. Holmes, and H. J. Guggenheim, *Phys. Rev. Lett.* **32**, 610 (1974); L. M. Holmes, J. Als-Nielsen, and H. J. Guggenheim, *Phys. Rev. B* **12**, 180 (1975).

⁸J. Als-Nielsen, L. M. Holmes, F. Krebs Larsen, and H. J. Guggenheim, *Phys. Rev. B* **12**, 191 (1975).

⁹G. Ahlers, A. Kornblitt, and H. J. Guggenheim, *Phys. Rev. Lett.* **34**, 1227 (1975).

¹⁰A reanalysis of the data published in Ref. 8 in terms of Eq. (3) yielded $B = 1.7 \pm 0.05$.

¹¹A. Aharony and B. I. Halperin, *Phys. Rev. Lett.* **35**, 1308 (1975).

¹²J. Als-Nielsen and I. Laursen, to be published.

¹³J. Als-Nielsen, *Phys. Rev.* **185**, 664 (1969); J. W. Essam and D. L. Hunter, *J. Phys. C* **1**, 392 (1968).

COMMENTS

Is the Axial Vector Charmed Meson Found?

Mahiko Suzuki*

Department of Physics and Lawrence Berkeley Laboratory, University of California, Berkeley, California 94720
(Received 26 August 1976)

It is argued that the charmed meson of $J^P = 1^+$ is produced copiously at the center-of-mass energy 4.028 GeV in electron-positron annihilation.

Goldhaber *et al.* have reported evidences for charmed mesons in a recent Letter,¹ in which they have shown, among others, the recoil mass spectrum against D^0 (\bar{D}^0). De Rújula, Georgi, and Glashow² have subsequently attributed the higher peak in the recoil mass spectrum to the kinematic reflection of the $D^{0*}(1^-)\bar{D}^{0*}(1^-)$ production. With more accurate values^{1,3} for the masses involved and with the actual beam energy ($\sqrt{s} = 4.028 \pm 0.005$ GeV), however, the ratio between the $D^0(0^-)\bar{D}^{0*}(1^-) + \bar{D}^0(0^-)D^{0*}(1^-)$ and $D^{0*}(1^-)\bar{D}^{0*}(1^-)$ production cross sections turns out to be

$$\sigma(D^{0*}\bar{D}^{0*}) / [\sigma(D^0\bar{D}^{0*}) + \sigma(\bar{D}^0D^{0*})] \simeq 0.052, \quad (1)$$

aside from possible form-factor effects, provided that the quark model based on statistical spin weight be valid.² The small number in (1) is due

to the vanishingly small Q value available for the $D^{0*}\bar{D}^{0*}$ channel. To explain the height of the higher recoil mass peak, this has to be close to the order of unity.

An alternative interpretation, probably more faithful to the experiment, is that the higher-recoil-mass peak is due to the production of $D^0(0^-)\bar{D}^{0*}(1^+)$ and its charge-conjugate state. In this case the mass is estimated from the momentum spectrum of D^0 (\bar{D}^0) to be 2.147 GeV. Since the production takes place in an s wave, the small Q value suppresses the $(0^-, 1^+)$ production less severely than the $(1^-, 1^-)$ production. This value of the 1^+ -charmed-meson mass is considerably smaller than 2.33 GeV for quark-mass spectroscopy⁴ and 2.5 GeV for the linearly-rising-potential model.⁵ It does not fit in linear mass